Journal of Hazardous Materials 476 (2024) 135102

Contents lists available at ScienceDirect

Journal of Hazardous Materials

journal homepage: www.elsevier.com/locate/jhazmat

Research Paper

Aquatic toxicity, bioaccumulation potential, and human estrogen/androgen activity of three oxo-Liquid Organic Hydrogen Carrier (oxo-LOHC) systems

Yohan Seol [a], Marta Markiewicz [a], Stephan Beil [a], Sara Schubert [b], Dirk Jungmann [b], Peter Wasserscheid [c,d,e], Stefan Stolte [a,*]

[a] Institute of Water Chemistry, Dresden University of Technology, 01069 Dresden, Germany
[b] Institute of Hydrobiology, Dresden University of Technology, 01069 Dresden, Germany
[c] Institute of Chemical Reaction Engineering, Friedrich Alexander University of Erlangen Nürnberg, Egerlandstraße 3, 91058 Erlangen, Germany
[d] Forschungszentrum Jülich GmbH, Helmholtz-Institute Erlangen-Nuremberg for Renewable Energy, 91058 Erlangen, Germany
[e] Forschungszentrum Jülich GmbH, Institute for a Sustainable Hydrogen Economy, 52428 Jülich, Germany

HIGHLIGHTS

- Oxo-LOHC compounds are generally baseline toxicants for tested aquatic organisms.
- Mixture toxicity of BP-based LOHC system is predicted well using a CA model.
- Oxo-LOHC compounds are unlikely to be bioaccumulative.
- Oxo-LOHC compounds did not show endocrine activity in YES/YAS assay.

GRAPHICAL ABSTRACT

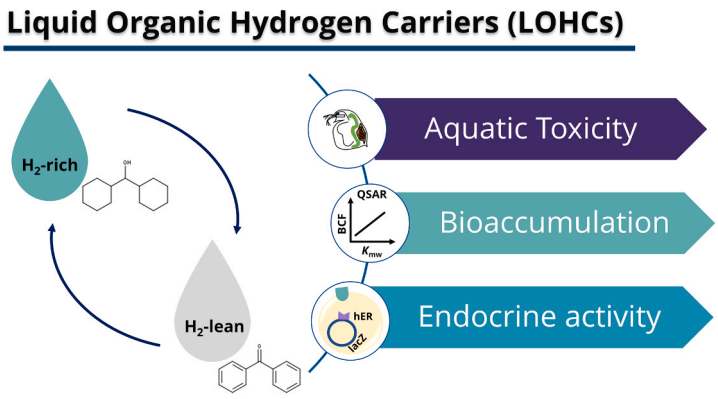

ARTICLE INFO

Keywords:
Hydrogen storage
Emerging pollutants
Ecotoxicity
Bioconcentration factor
Yeast-based reporter gene assay

ABSTRACT

The Liquid Organic Hydrogen Carrier (LOHC) technology offers a technically attractive way for hydrogen storage. If LOHC systems were to fully replace liquid fossil fuels, they would need to be handled at the multi-million tonne scale. To date, LOHC systems on the market based on toluene or benzyltoluene still offer potential for improvements. Thus, it is of great interest to investigate potential LOHCs that promise better performance and environmental/human hazard profiles. In this context, we investigated the acute aquatic toxicity of oxygen-containing LOHC (oxo-LOHC) systems. Toxic Ratio (TR) values of oxo-LOHC compounds classify them baseline toxicants ($0.1 < TR < 10$). Additionally, the mixture toxicity test conducted with *D. magna* suggests that the overall toxicity of a benzophenone-based system can be accurately predicted using a concentration addition model. The estimation of bioconcentration factors (BCF) through the use of the membrane-water partition coefficient indicates that oxo-LOHCs are unlikely to be bioaccumulative ($BCF < 2000$). None of the oxo-LOHC compounds exhibited hormonal disrupting activities at the tested concentration of 2 mg/L in yeast-based

* Corresponding author.
E-mail address: stefan.stolte@tu-dresden.de (S. Stolte).

https://doi.org/10.1016/j.jhazmat.2024.135102
Received 28 March 2024; Received in revised form 24 June 2024; Accepted 3 July 2024
Available online 4 July 2024

reporter gene assays. Therefore, the oxo-LOHC systems seem to pose a low level of hazard and deserve more attention in ongoing studies searching for the best hydrogen storage technologies.

1. Introduction

Hydrogen, known for its high gravimetric energy density (120 MJ/kg) [1], has emerged as a potential secondary energy vector – one that is nearly emission-free if produced using renewable energy. However, the low volumetric density of hydrogen (0.091 g/L) necessitates either pressurized gaseous hydrogen or cryogenic liquid hydrogen for which a significant investment in the infrastructure is a key hurdle [2]. As a viable solution, Liquid Organic Hydrogen Carrier (LOHC) systems, consisting of a pair of H_2-lean and H_2-rich compounds, have gained increasing attention in recent years. In such systems, hydrogen is first bound to the H_2-lean form of a carrier molecule and subsequently released from the H_2-rich form through catalytic (de)hydrogenation processes (Fig. 1) [3]. A striking advantage of LOHC systems is that hydrogen, covalently bound to the LOHC compound, can be stored as a liquid under ambient conditions. This is key as our current fossil fuel-based infrastructure can simply be adapted for storage and distribution of LOHCs, and thus of hydrogen [4]. Recently, in the Netherlands, the Port of Rotterdam Authority has announced plans to import 20 million tons of hydrogen by 2050, utilizing the toluene/methylcyclohexane (TOL/MCHEX) LOHC system (Fig. 2A) [5]. In Germany, the first hydrogen-refuelling station was established utilizing the benzyltoluene/perhydro-benzyltoluene (H0-BT/H12-BT)-based LOHC system (Fig. 2B) for mobility applications [6]. Furthermore, a megawatt LOHC/fuel-cell based propulsion system is being developed for maritime transport [7].

A recent development in the field of LOHC systems is oxygen-containing LOHC (hereafter denoted as 'oxo-LOHC') systems, which offer a high hydrogen storage capacity coupled with low dehydrogenation temperatures [8]. The latter facilitates the use of waste heat generated by the energetic utilization of the released hydrogen (e.g. in a fuel cell or a combustion engine) for the endothermal hydrogen release from the LOHC system [9]. Herein, three oxo-LOHC systems were investigated, namely benzophenone/dicyclohexylmethanol (H0-BP/H14-BP), methyl-benzophenone/perhydro-methylbenzophenone (H0-MBP/H14-MBP), and acetophenone/cyclohexylethanol (H0-ACP/H8-ACP). Recently, the H0-BP/H14-BP LOHC system has been shown to release the first H_2 molecule from H14-BP under mild conditions (170 °C) [8], which is advantageous for the aforementioned heat integration when compared to other LOHC that typically operate at temperatures above 250 °C [3,10,11]. In addition, the H0-BP/H14-BP LOHC system (Fig. 2D) is characterized by a high gravimetric hydrogen storage capacity (7.19 wt% or 2.39 kWh/kg based on the lower heating value of the reversibly bound hydrogen), which outperforms well-known LOHC systems, namely the TOL/MCHEX and H0-BT/H12-BT LOHC systems (both by 17 %) or N-ethylcarbazole/perhydro-N-ethylcarbazol (H0-NEC)/H12-NEC (by 23 %) [8].

The successful implementation of LOHC systems – even for niche applications – raises concerns with regard to their environmental safety and their threat to human health in the event of release during use or

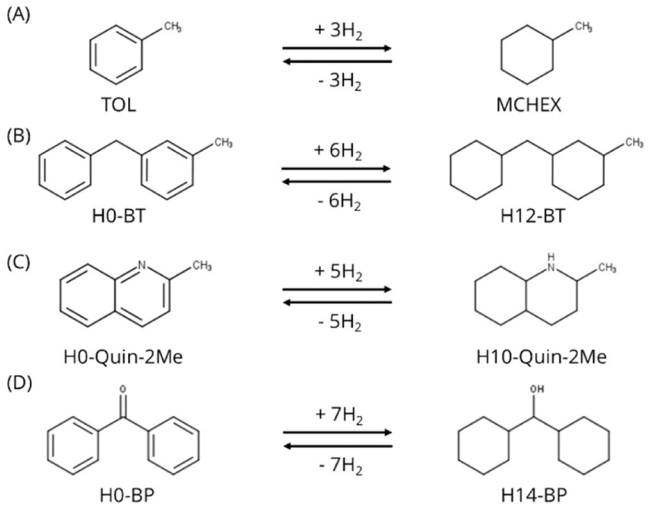

Fig. 2. Reversible hydrogen storage in four LOHC systems. The number of H_2 shows the added or removed hydrogens from each form through catalytic hydrogenation or dehydrogenation process. Abbreviation: toluene (TOL), methylcyclohexane (MCHEX), benzyltoluene (H0-BT), perhydro-benzyltoluene (H12-BT), quinaldine (H0-Quin-2Me), perhydro-quinaldine (H10-Quin-2Me), benzophenone (H0-BP), and dicyclohexylmethanol (H14-BP).

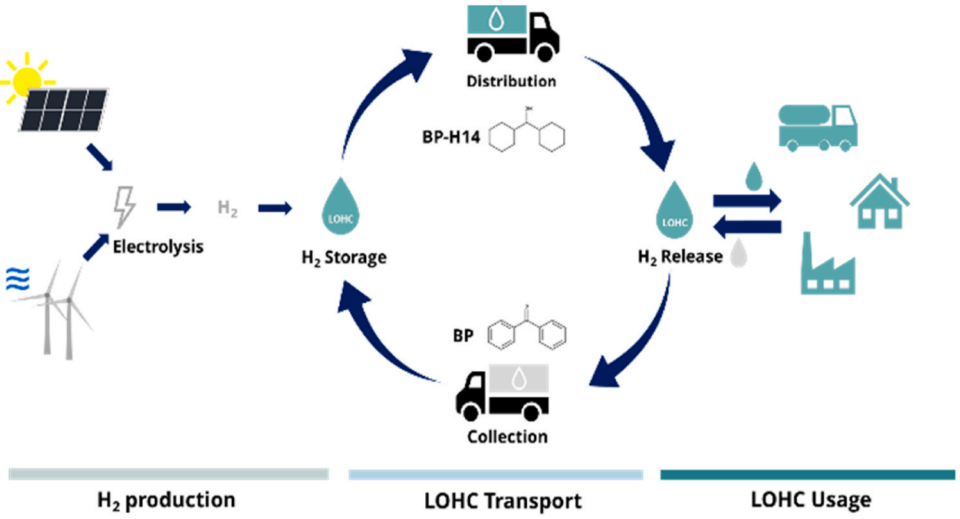

Fig. 1. The benzophenone/dicyclohexylmethanol LOHC system showing the process of storing and using hydrogen.

transport. Additionally, the EU Strategy for Sustainability promotes the use of chemicals which are safe and sustainable by design [12]. In light of these considerations, the potential environmental hazards of oxo-LOHCs need to be assessed at this early stage of technological development to ensure that efforts to achieve climate goals do not have negative impacts in other areas (the so-called regrettable substitution). Various systems, including quinaldine, indole-, alkylcarbazole-, benzene-, toluene-, benzyltoluene-, and dibenzyltoluene-based LOHCs have already been investigated in this regard [13–16]. Endocrine disruption is another significant concern, as chemicals can mimic natural hormones, potentially disrupting the hormonal systems of humans and animals. These effect include decreased reproductive output, delayed or altered development, and occurrence of certain diseases [17].

In this study, we investigated aquatic toxicity of oxo-LOHC systems because benzophenone and its derivatives, such as mono- and dihydroxybenzophenones, some of which are used as UV filters in sunscreen products and in food packaging, are known to be toxic to aquatic organisms [18,19]. We hypothesized that the aquatic toxicity of oxo-LOHCs would be caused by a hydrophobicity-driven disturbance of cell membrane function - known as baseline toxicity. To verify this mode of action the octanol-water partition coefficient (log K_{OW}) was predicted using the COnductor like Screening MOdel for Realistic Solvation (COSMO-RS) and used to estimate the baseline toxicity via established Quantitative Structure-Activity Relationship (QSAR) models. To investigate a broad environmental impact, we included three aquatic organisms at different trophic levels: luminescent marine bacteria (*Aliivibrio fischeri*), unicellular limnic algae (*Raphidocelis subcapitata*), and water invertebrate (*Daphnia magna*). Additionally, the toxicities of the oxo-LOHC systems were compared with those of two well-known LOHC systems (Fig. 2A and C).

Secondly, we investigated the mixture toxicity of six known components of the H0-BP/H14-BP LOHC system to *Daphnia magna* because it is possible that oxo-LOHCs, as technical grade products, will contain mixtures of various hydrogenated and dehydrogenated forms of a specific LOHC system which might be released into the environment. In the form of a mixture, we assumed that oxo-LOHC compounds would behave in a concentration-additive manner if they were baseline toxicants. To test this hypothesis, a concentration addition model was used and compared with experimental results. On the other hand, the membrane-water partition coefficient (log K_{MW}) of oxo-LOHC compounds was determined to assess the membrane affinity of these compounds and to estimate their bioconcentration factor (BCF).

Lastly, we investigated the (anti)estrogenic and (anti)androgenic potentials of oxo-LOHCs using yeast-based reporter gene assays because benzophenone showed weak estrogenic activity in the YES test with an EC_{50} of 1.82 mg/L [20] and hydroxybenzophenones were identified as one of the structural alerts for endocrine activity [21–23]. Therefore, we assumed that compounds with benzophenone-based structure may induce endocrine activity.

We aim to provide the first hazard assessment of oxo-LOHC systems to support the development of responsible and sustainable LOHC technologies, technologies that align with environmental considerations while also seeking high levels of operational effectiveness in their hydrogen storage and transportation task.

2. Materials and methods

2.1. Chemicals

Benzophenone (H0-BP; 99.8 %) and 2-hydroxy-4-methoxybenzophenone, commonly referred to as benzophenone-3 (BP-3; ≥99.9 %), were purchased from HPC Standards GmbH, and acetophenone (H0-ACP; 99 %) was purchased from Sigma-Aldrich (Merck KGaA). Benzhydrol (H2-BP), cyclohexylphenylketone (H6-BP), cyclohexylphenylmethanol (H8-BP), dicyclohexylketone (H12-BP), dicyclohexylmethanol (H14-BP), 2-methylbenzophenone (H0–2-MBP), 3-methylbenzophenone (H0–3-MBP), 4-methylbenzophenone (H0–4-MBP), 4-methyl-dicyclohexylmethanol (H14–4-MBP), and 1-cyclohexylethanol (H8-ACP) were obtained from the University of Erlangen, Germany with a purity > 97 % [8]. Naphthalene and pyrene were purchased from Fluka (≥99 %). Dithiothereitol (DTT), 4-hydroxytamoxifen (OHT), and flutamide (FLU) in analytical grade were purchased from Sigma-Aldrich (Merck KGaA). Analytical grade 4-methylum-belliferyl-β-D-galactopyranoside (MUG) was purchased from Carl Roth GmbH. 17β-estradiol (E2) and testosterone (T) were purchased from Merck KGaA (>97 %).

2.2. Instrumental analysis and sample preparation

The analysis of H12-BP, H14-BP, H14–4-MBP, and H8-ACP was carried out using GC-MS. An Agilent 7890A gas chromatograph equipped with a Restek Rxi®− 5 ms column (30 m x 0.25 mm, 0.25 μm film thickness) was coupled to an Agilent 5975 C mass spectrometer. Using an automatic injection system (G6500-CTC), 1 μL liquid samples were injected with an inlet temperature of 250 °C. Split injection (5:1 split ratio) and splitless injection were used for toxicity samples, while pulsed splitless injection was used for TRANSIL samples (K_{MW}). The oven program was as follows: 2 min hold at 55 °C, followed by a temperature ramp at 50 °C/min to 320 °C and finally 1 min hold at 320 °C. The GC-MS was operated in electron ionization mode with the energy at 70 eV, while the transfer line was set at 315 °C and quadrupole at 180 °C. The carrier gas (helium) flow rate was set to 1.6 mL/min. The calibration standards for GS-MS analysis of the toxicity test samples ranged from 1 mg/L to 10 mg/L and were measured with split injections (H12-BP, H14-BP, and H14–4-MBP) and splitless injection (H8-ACP). The calibration standards for GC-MS analysis of the TRANSIL samples ranged from 10 μg/L to 250 μg/L and were measured using pulsed splitless injection mode. The sample preparation for GC-MS analysis involved solvent extraction. Specifically, 2 mL of the sample was transferred into a 20 mL glass vial with a teflon screw cap, followed by extraction with 2 mL of hexane by shaking for 30 min at 200 rpm (HS501 D, Janke & Kunkel GmbH). After shaking, the hexane phase was transferred into a 4 mL glass vial and then dried with anhydrous sodium sulfate. Afterwards, the 1 mL of hexane extract was transferred into a 1.5 mL glass vial and 25 μL naphthalene (internal standard; 1000 μg/L in hexane) was added. For TRANSIL samples, pyrene was used as a surrogate standard for the extraction of H12-BP, H14-BP, and H14–4-MBP. The extraction rates of oxo-LOHCs and pyrene were higher than 87 % (Table S1). The Limits of Detection (LOD) and Limits of Quantification (LOQ) are shown in the supplementary information (Table S2).

An ExionLC™ liquid chromatography system, coupled with a tandem mass spectrometry (SCIEX Triple Quad™ 4500 MS/MS), was used to determine the concentration of H0-BP, H2-BP, H6-BP, H8-BP, H0–2-MBP, H0–3-MBP, and H0–4-MBP in samples. LC-MS/MS was operated in positive electrospray ionization mode. A Kinetex EVO C18 column (100 Å, 100 ×2.1 mm, 5 μm particle size, Phenomenex) was used for the chromatographic separation. The column oven was set at 40 °C. Eluent A consisted of 950 mL H_2O, 50 mL acetonitrile, and 150 μL formic acid, while eluent B consisted of 1000 mL Acetonitrile and 150 μL HCOOH. The elution gradient was set as follows: 0.0–0.5 min, 20 % B; 0.5–3.5 min, 98 % B; 3.5–5.0 min, 98 % B; 5.00–5.02 min, 20 % B; 7.0 min, 20 % B. The flow rate of the eluent was 0.4 mL/min and the injection volume was 3 μL. The calibration ranged from 10 μg/L to 1000 μg/L. The aqueous sample (4 mL) was mixed with 4 mL of 50:50 = H_2O:MeOH and then BP-3 (2-hydroxy-4-methoxybenzophenone; internal standard) was added (200 μL). The sample was then filtered with a regenerated cellulose syringe filter (0.2 μm pore size, Macherey-Nagel GmbH). The first 5 mL of filtered test solution were discarded and the following 1 mL of filtered solution was used for the analysis. LOD and LOQ are given in the supplementary information (Table S3).

2.3. Ecotoxicity test (A. fischeri, R. subcapitata, and D. magna)

The *Aliivibrio fischeri* (Luminescent marine bacteria) acute luminescence inhibition test was performed according to DIN 11348-2. Freeze-dried bacteria from a commercial test kit (LUMIStox; Hach Lange GmbH) were reconstituted in the reactivation solution for 15 min at 15 °C. Subsequently, the initial luminescence of bacteria was measured using a luminometer (LUMIStox 300, Dr. Lange). A suspension of bacteria (500 μL) was mixed with 500 μL of test sample prepared in phosphate buffer including 2 % NaCl (2 g NaCl /100 mL phosphate buffer; pH=7.0). This was incubated for 30 min at 15 °C and the luminescence was measured again. The bacteria were exposed to five different concentrations of test compounds (in duplicate). At least three negative controls (only medium) and two/three positive controls (sodium chloride 7.5 g/L) were included in every test. Three independent tests were conducted. Since exposure duration was only 30 min and preliminary analysis confirmed stable chemical exposure over the test period, the EC_{50} values were calculated based on the nominal concentration. A concentration-response analysis was performed for most compounds except H6-BP, H14-BP, and H14-MBP for which only limit tests were performed - at the saturation level of each compound in the test medium (see the legend in Table 1).

The algae growth inhibition test was conducted according to OECD 201. Green algae, *Raphidocelis subcapitata*, was also obtained from the Culture Collection of Algae at Göttingen University (SAG) in Germany. *R. subcapitata* was cultured in OECD medium (OECD TG 201; pH = 8.1) at 21 °C under the 16 h:8 h (light:dark) cycle. *R. subcapitata* was exposed to six different concentrations of the test compound, each in three replicates accompanied by six replicates for control samples (only medium). The number of algal cells was determined using a CASY® Model TTC cell counter and used for the calculation of growth rate. Initial algae cell counts were 6 000 cells/mL. The final cell density in the treated samples was recorded after 72 h. Cell density was recorded daily in the control samples (i.e. after 24 h, 48 h, and 72 h). Three independent experiments were conducted for every test substance. The pH of the test solutions was measured at the beginning and at the end of each test, and it was generally within the criteria range. 3,5-dichlorophenol was used as a reference substance and was tested two times per year.

The *Daphnia magna* acute immobilization test was conducted according to OECD 202. *D. magna* was obtained from Biochem agrar GmbH in Leipzig, Germany. Daphnids were obtained from in-house culture maintained in M4 medium at 20 °C under a 16 h:8 h (light:dark) photoperiod. Daphnids were fed three times a week with live *Desmodesmus subspicatus* (0.2 mg C/daphnid/day). The *D. subspicatus* was purchased from SAG and has been cultured in the lab. In addition, daphnids were fed once a week with Tetra Goldfish Crisps from Tetra GmbH and with spirulina powder from Steinberger GmbH. Neonates (< 24 h) were exposed to five different concentrations of each compound for 48 h. Test solutions were prepared in the medium (pH = 7.8) consisting of calcium chloride (293.8 mg/L), magnesium sulfate (123.3 mg/L), sodium bicarbonate (64.8 mg/L), and potassium chloride (5.8 mg/L). A negative control (only medium) was included in each test. After 24 and 48 h, immobilization of neonates was recorded. There were four replicates in each treatment and each replicate included five neonates. Three independent experiments were conducted for every test substance. The pH of the test solutions was measured before and after the test, and it did not deviate significantly by the end of the test. Potassium dichromate and diclofenac salt were used as reference substances and were tested two times per year.

The test concentration was determined based on either literature values or estimated EC_{50} values from baseline toxicity QSAR models (see Fig. 3). Based on the range-finding test, the exposure range was refined to encompass the inhibition range (0–100 %). The concentration of oxo-LOHC compounds in test samples from toxicity tests was measured at the beginning and the end of the test using either GC/MS or LC-MS/MS. In the first test of each compound, all test concentrations during the test period were measured and a deviation of under 20 % was confirmed. Afterwards only the lowest and the highest concentrations of the test samples were measured. The half maximal effective concentration (EC_{50}) of LOHC compounds for three aquatic organisms was calculated using GraphPad Prism version 9.5.0. For algae EC_{50}, the inhibition of the 72 h average growth rate was calculated. Note that the EC_{50} values of oxo-LOHCs from *D. magna* and *R. subcapitata* tests were calculated using measured concentrations that were kept within ± 20 % of the initial concentration over the test period (Table S4 and S5).

2.4. Determination of membrane-water partition coefficient (K_{MW}) using TRANSIL

Solid-Supported Lipid Membranes (SSLM) composed of phosphatidylcholine (POPC, 12 μL/mL suspension in phosphate buffer saline) acquired commercially (TRANSIL® Intestinal Adsorption (Sovicell, Leipzig)) was used to determine K_{MW} values of LOHCs. Test solutions were prepared in dimethyl sulfoxide (DMSO) and then diluted with phosphate-buffered saline (PBS, pH 7.4; Thermo Fisher Scientific) to the desired test concentration (< 1 % DMSO). Five different volumes of SSLM were added to the test samples in 1.5 mL glass vials and the samples were shaken for 30 min at 25 °C and 700 rpm on the shaker (KS 125 basic, Janke & Kunkel GmbH). For the negative control, the same amount of PBS buffer was added to the sample instead of SSLM suspension. Afterward, the samples were centrifuged at 10,000*g* for 10 min at room temperature. The supernatant from the samples was extracted with hexane for GC/MS analysis or diluted with 50:50 H_2O:MeOH for LC-MS/MS to determine the amount of test compound which was not bound by the SSLM (C_{PBS}). Negative controls without SSLM were processed in the same way to determine nonspecific binding or losses (C_{total}). C_{SSLM} (the lipid-bound concentration) was determined using the following (Eq. (1)) [24]:

$$\log K_{MW} = \log\left(\frac{V_{total}}{V_{lipid}} \bullet \frac{n_{total} - n_{supernatant}}{n_{total}}\right) \quad (1)$$

The linear regression analysis of C_{PBS} vs. C_{SSLM} was performed using the LINEST function in Microsoft Excel (Fig. S1).

2.5. Prediction of the octanol-water partition coefficient (log K_{OW}) and membrane-water partition coefficient (log K_{MW}) using COSMO

log K_{OW} and log K_{MW} were predicted by the COnductor like Screening MOdel for Realistic Solvation (COSMO-RS). 3D structure files of the studied oxo-LOHC compounds were obtained via density functional theory (DFT)/COSMO calculations using COSMOtherm, version 18.0.2, in combination with TURBOMOLE [25–27]. For all of these calculations, Becke-Perdew density functional theory, a triple-zeta valence polarization basis set with additional diffuse basis functions and fine grid marching tetrahedron cavity construction (TZVPD-FINE) were applied [28,29]. Since COSMO-RS theory is able to predict chemical potentials and partitioning coefficients between pure phases, log K_{OW} values can be easily obtained based on DFT/COSMO calculations of water, octanol and the oxo-LOHC compounds. However, membrane partitioning is more complicated due to the complex structure of lipid bilayers. The software extension COSMOmic allows the prediction of membrane partitioning coefficients based on a previously published 1-palmitoyl-2-oleoyl-sn-glycero-3-phosphocholine (POPC) micelle structure [30,31]. POPC was chosen in order to allow for comparison with the TRANSIL studies which were performed using this lipid.

2.6. Mixture toxicity test (D. magna)

Six oxo-LOHC compounds were used in this mixture toxicity test (H0-BP, H2-BP, H6-BP, H8-BP, H12-BP, H14-BP). Concentrations corresponding to 5 %, 20 %, 40 %, 50 %, 60 %, 80 %, 90 %, 95 % effect for

each compound were calculated from concentration-response curves for the single compound using Graphpad. The concentrations corresponding to a 100 % effect, at which all daphnids tested would be immobilized, was set to 10 % higher than the concentration corresponding to 95 % effect because EC_{100} cannot be mathematically calculated. For example, EC_{95} of H0-BP is 24.3 mg/L and EC_{100} of H0-BP is estimated to 26.7 mg/L which is 2.4 mg/L higher than EC_{95}. Then, effective concentrations of the mixture corresponding to the effect of 5 %, 10 % and etc. (EC_{xmix}) were calculated using the concentration addition (CA) model (Eq. (2)) [32] and prepared for the toxicity test. Herein, n denotes the number of compounds in the mixture, p_i denotes the proportion of *i*th compound in the mixture ($p_i = c_i/c_{total}$). EC_{xmix} is the joint effect at the total concentration of the mixture. EC_{xi} is the x% effect of *i*th compound when applied in isolation. Two independent toxicity tests were conducted as described for the *D. magna* acute immobilisation test.

$$ECx_{mix} = \left(\sum_{i}^{n} \frac{p_i}{ECx_i} \right)^{-1} \quad (2)$$

Another concept is independent action (IA) where compounds of a given mixture act independently, i.e. having different sites of action (e.g. molecular acceptor). The IA model was calculated according to Eq. (3) [32].

$$E(c_{mix}) = 1 - \prod_{i=1}^{n} [1 - E(c_i)] \quad (3)$$

The Index of Prediction Quality (IPQ; Eq. (4)) was used to assess the difference between the experimental result and the CA model [33,34]. If IPQ_{CA} is zero, the prediction agrees ideally with the experimental value.

$$If\ EC_{50,CA} > EC_{50,\exp},\ then\ IPQ_{CA} = \frac{EC_{50,CA}}{EC_{50,\exp}} - 1,$$

$$else\ IPQ_{CA} = 1 - \frac{EC_{50,CA}}{EC_{50,\exp}} \quad (4)$$

2.7. Yeast-based reporter gene assays

Recombinant yeast strains were used for each yeast endocrine screening assay. Human Estrogen Receptor (hERα) is integrated into yeast cells in the Yeast Estrogen Screen (YES) and in the Yeast Anti-Estrogen Screen (YAES). Human Androgen Receptor (hAR) is integrated into yeast cells in the Yeast Androgen Screen (YAS) and in the Yeast Anti-Androgen Screen (YAAS). The test was conducted according to ISO 19040-1 and as described elsewhere [23]. In brief, once the estrogen (or androgen) agonist binds to the estrogen (or androgen) receptor in YES (or YAS), estrogen-responsive elements trigger expression of the lacZ gene, which leads to production of β-galactosidase. The amount of β-galactosidase produced is proportional to the level of activation. When the β-galactosidase is secreted to the medium, it cleaves the 4-methylum-belliferyl-β-D-galactopyranoside (MUG) into β-D-galactose and 4-methylumbelliferone (4-MU). The blue fluorescence of 4-MU was measured (λ_{ex} = 360 nm, λ_{em} = 485 nm). In the anti-activity assays, 17β-estradiol or testosterone were added to the media and the decrease in 4-MU fluorescence was measured as the antagonist inhibits the binding of 17β-estradiol (or testosterone) to each receptor.

Test stock solutions of oxo-LOHC compounds (C = 1000 mg/L) were prepared in methanol and positive controls were prepared in ethanol. Test stock solutions were serially diluted in methanol to the final test concentration (2 mg/L) and positive control stocks were diluted in ethanol. Blank (without yeast and the test compound), negative control (NC; without the test compound), and solvent control (SC; without the test compound) were included. All test compounds, blanks, and controls were measured in pseudo-octuplicates. Yeast cells were cultured for two to three days at 30 °C and 450 rpm to obtain a sufficient yeast density - assessed based on optical density measured at 595 nm. Water and samples (including blanks) were transferred to the 96 well plate (optically transparent and flat-bottomed; Thermo Scientific™) and then yeast suspensions were transferred to the plate. Afterward, the mixture of Lac-Z-buffer, dithiothreitol (DTT), and MUG was added and incubated for one hour at 30 °C and 450 rpm. The fluorescence was read at λ_{ex} = 360 nm and λ_{em} = 485 nm. As positive controls, 17β-estradiol (E2) in YES, testosterone (T) in YAS, 4-hydroxytamoxifen (OHT) in YAES, and flutamide (FLU) in YAAS were used for the calibration curve, which was fitted using GraphPad Prism version 9.5.0. (Fig. S2). The bioanalytical equivalents (BEQ), which are E2-equivalents (E2-EQ) in YES and T-equivalents (T-EQ) in YAS, were used to benchmark the strength of the effect. In the antagonistic test, OHT-EQ and FLU-EQ were used. Two independent tests were conducted for oxo-LOHC compounds. The calculation of BEQs and LOQs is shown in the supplementary information (see Text S1).

3. Results and discussion

3.1. Acute aquatic toxicity

Concentration-response curves for the oxo-LOHC compounds in three tests are shown in Figs. S3-S5. EC_{50} values in μmol/L are shown in Table S6. In the *A. fischeri* test, the EC_{50} values for the oxo-LOHC compounds range from 5.0 mg/L to 81.3 mg/L (Table 1). Oxo-LOHC compounds with two rings were more toxic to both *R. subcapitata* and *D. magna* (EC_{50} = 0.146 – 38.1 mg/L) than H0-ACP and H8-ACP (EC_{50} = 157 - 529 mg/L). Among the oxo-LOHC compounds with two rings, H0–3-MBP and H0–4-MBP exhibited particularly high toxicity towards algae with EC_{50} values lower than 1 mg/L, corresponding to acute aquatic toxicity category 1 (“very toxic to aquatic life”; red) according to the Globally Harmonized System of Classification and Labelling of Chemicals (GHS) [43]. The remaining compounds belong to either acute 2 (“toxic to aquatic life”; orange) or acute 3 (“harmful to aquatic life”; yellow) based on algae and water flea test results. The EC_{50} values for benzophenone against *R. subcapitata* and *D. magna* are 2.7 mg/L and 11.1 mg/L respectively, which is in good agreement with the previously reported values (3.5 mg/L [44] and 9.5 mg/L [19], respectively). The EC_{50} values measured in *R. subcapitata* and *D. magna* tests for H0-ACP and H8-ACP are higher than the last threshold in the GHS (100 mg/L; green), thus these compounds would not require labelling with respect to their aquatic toxicity.

In the H0-BP/H14-BP LOHC system, H2-BP showed the lowest toxicity across all species and H14-BP was the most toxic towards *D. magna*, which can be explained by the difference in their structure and corresponds to their different hydrophobicities. In addition, the difference in EC_{50} values within one oxo-LOHC system is less than one order of magnitude in the *R. subcapitata and D. magna* tests, indicating that the hydrogenation or dehydrogenation processes do not significantly alter the toxicity of the compound within the same system. The impacts of the presence and position of the methyl group within the benzophenone structure were investigated by comparing the H0-BP/H14-BP LOHC system to the MBP-based LOHC systems. Interestingly, the methyl group at the ortho and para positions did not significantly influence the toxicity in the algae test, while the methyl group in the meta position significantly increased toxicity compared to benzophenone. Specifically, the EC_{50} value decreased to less than one-tenth of that of benzophenone. On the other hand, in the *A. fischeri* and *D. magna* tests, the presence of a methyl group, regardless of its position, did not significantly increase the toxicity compared to benzophenone. In addition, except for H0–2-MBP and H0–3-MBP, all tested compounds showed similar levels of toxicity across three different trophic levels, with EC_{50} values within one order of magnitude. In the case of H0–3-MBP and H0–4-MBP, *R. subcapitata* is the most sensitive of tested species (the lowest EC_{50} values) and therefore dictates the overall GHS classification. Thus, the 3-MBP- and 4-MBP-based LOHC systems are classified as acutely toxic to aquatic life

Table 1
EC_{50} values (including 95 % confidence intervals) of LOHC systems from three toxicity tests as well as the corresponding octanol-water partition coefficients and lipid membrane-water partition coefficients (measured, +/-standard error). The abbreviations for the chemical names indicate the basic structure of the compound along with the number of hydrogen atoms added to the structure as compared to the H_2-lean form.

Chemical name[a]	Structure	CAS No.	log K_{OW}	log K_{MW}	*A. fischeri* EC_{50} (mg/L)	*R. subcapitata* EC_{50} (mg/L)	*D. magna* EC_{50} (mg/L)
H0-BP		119-61-9	3.18[b]	3.13±0.06	16.4 (15.0-17.8)	2.65 (2.37-2.98)	11.1 (10.2-12.0)
H2-BP		91-01-0	2.67[b]	2.88±0.02	81.3 (79.2-83.5)	17.4 (15.3-20.4)	38.1 (37.4-38.8)
H6-BP		712-50-5	3.68[c]	3.88±0.04	> 4.2[d]	4.38 (4.01-4.81)	6.26 (5.91-6.61)
H8-BP		945-49-3	3.54[c]	3.33±0.03	25.0 (24.0-26.0)	12.1 (10.4-14.2)	21.7 (21.0-22.3)
H12-BP		119-60-8	3.95[c]	3.91±0.06	5.66 (5.2-6.3)	11.2 (10.4-12.0)	5.52 (5.17-5.93)
H14-BP		4453-82-1	4.28[c]	3.77±0.11	> 1.5[e]	3.40 (3.18-3.64)	3.97 (3.33-4.68)
H0-2-MBP		131-58-8	3.62[c]	3.43±0.04	17.1 (16.0-18.3)	1.22 (1.09-1.39)	10.7 (10.4-10.9)
H0-3-MBP	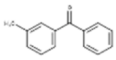	643-65-2	3.63[c]	3.54±0.03	16.2 (15.0-17.6)	0.15 (0.14-0.15)	5.93 (5.69-6.19)
H0-4-MBP	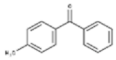	134-84-9	3.45[c]	3.67±0.03	4.96 (4.53-5.50)	0.62 (0.59-0.64)	6.21 (6.07-6.39)
H14-4-MBP	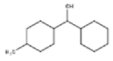	n.a.	4.68[c]	3.84±0.07	> 1.3[e]	3.27 (3.00-3.62)	2.72 (2.54-2.90)
H0-ACP		98-86-2	1.58[b]	-	28.7 (26.8-30.8)	199 (184-216)[f]	162-529[g]
H8-ACP		1193-81-3	2.24[c]	-	68.9 (65.9-72.1)	268 (245-293)	157 (151-162)
TOL		108-88-3	2.73[b]	n.a.	21.4[h]	12.5[i]	5-21[j,k]
MCHEX		108-87-2	3.61[b]	n.a.	3.55[h]	0.134[l]	0.326[l]
H0-Quin-2Me		91-63-4	2.45[m]	n.a.	19 (16-22)[n]	43[n]	56 (54-59)[o]
H4-Quin-2Me		1780-19-4	3.04[m]	n.a.	7.4 (6.2-8.9)[n]	17 (14-20)[n]	2.7 (2.3-3.2)[o]
H10-Quin-2Me		20717-43-5	3.25[m]	n.a.	>306[n,p]	52[n]	155 (120-191)[n]

Colour code [43]

Acute 1	Acute 2	Acute 3	not labelled
EC_{50} ≤ 1 mg/L	1 mg/L< EC_{50} ≤ 10 mg/L	10 mg/L< EC_{50} ≤ 100 mg/L	EC_{50} > 100 mg/L

[a] The full name of the respective oxo-LOHC compounds is given in the chemical information section of the materials and methods. Abbreviation for the other compounds: toluene (TOL), methylcyclohexane (MCHEX), benzyltoluene (H0-BT), perhydro-benzyltoluene (H12-BT), quinaldine (H0-Quin-2Me), tetrahydro-quinaldine (H4-Quin-2Me), and decahydro-Quinaldine (H10-Quin-2Me). [b] Experimental log K_{OW} values from Ref. [35]. [c] log K_{OW} values predicted using COSMO-RS at TZVPD-FINE level. [d] exact EC_{50} could not be calculated because approximately 50 % inhibition was achieved at the solubility limit. [e] EC_{50} could not be calculated because approximately 10 % inhibition was observed at the solubility limit. [f] exposure duration was 48 h. Ref. [36]. [g] LC_{50} from Ref. [37,38]. [h] Predicted values using a baseline QSAR model in Fig. 2 (A). [i] According to Ref. [39]. [j] LC_{50} values are included (5 mg/L and 12 mg/L) according to Ref. [37,38,40,41]. [k] The lowest EC_{50} value was used for the colour code. [l] Ref. from [42]. [m] predicted values using COSMO-RS according to Ref. [16]. [n] According to Ref. [15]. [o] According to Ref. [13]. [p] Luminescence inhibition did not reach 40 % at the highest concentration in the test. *Chemical structures were drawn using Marvinsketch v22.22. n.a. – data not available.

– category 1, while BP- and 2-MBP-based LOHC systems fall into category 2 of acute aquatic toxicity. Lastly, the H0-ACP/H8-ACP LOHC system cannot be categorized (EC_{50} > 100 mg/L).

3.2. Acute aquatic toxicity in comparison with other LOHC systems

To put the ecotoxicity of oxo-LOHC compounds into perspective, we chose two other LOHC systems for which similar data were available for a comparative assessment. These benchmark systems were the hydrocarbon-based toluene/methylcyclohexane (TOL/MCHEX) system used commercially by the Chiyoda corporation [45,46] and the N-heterocyclic, Quinaldine-based (H0-Quin-2Me/H10-Quin-2Me) LOHC system (which has the literature-known advantage of a comparatively low dehydrogenation temperature) [1,47]. The EC_{50} or LC_{50} values of toluene against *D. magna* range from 5 to 21 mg/L [37,38,40,41], while the EC_{50} for *R. subcapitata* is reported as 12.5 mg/L [39]. On the other hand, for methylcyclohexane (MCHEX; the fully hydrogenated form of toluene), EC_{50} values of 0.326 mg/L for *D. magna* and 0.134 mg/L for *R. subcapitata* were reported (Table 1) [42]. These values mandate classifying MCHEX as very toxic to aquatic organisms according to the GHS ("acute 1″). Based on the lowest EC_{50} values, the toxicity of the TOL/MCHEX LOHC system is comparable to that of the 3-MBP and 4-MBP-based LOHC systems (both acute aquatic toxicity category 1), while the BP- and especially the ACP-based systems are less toxic. In comparison to the Quinaldine-based system, benzophenone- and 2-MBP-based systems have similar or higher toxicity towards *R. subcapitata* and *D. magna*, as EC_{50} values of the Quinaldine-based system range from 2.7 mg/L to 155 mg/L [13,15]. This leads to this system being classified as category "acute 2″ according to the GHS, if the lowest EC_{50} is taken into account. In this regard, 3-MBP and 4-MBP-based systems can be considered more toxic than the Quinaldine-based system. Among the LOHC systems discussed, the order of toxic potency can be specified as follows based on the lowest EC_{50} value of their constituent compounds: TOL ≈ 3-MBP, 4-MBP > Quinaldine ≈ BP, 2-MBP > ACP. While oxo-LOHC systems still require significant technological development, a comparison of their toxicity with two benchmark systems reveals a clear advantage of low aquatic toxicity for the ACP-based system. It should be noted that other aspects (e.g. chronic toxicity, the bioaccumulation potential, mobility in soils etc.) should be taken into account for a comprehensive environmental hazard assessment [48,49].

3.3. Prediction models and mode of toxic action

The growing number of new chemicals outpaces the chemical risk assessment, raising concerns for chemical safety [50]. As a consequence, it is difficult to assess all of the new chemicals with conventional *in vivo* methods in a timely manner [51]. In this context, prediction models offer a promising approach for a preliminary assessment, which provides insights into the potential hazard of chemicals. In the following sections, we have employed different prediction models to assess single-compound toxicity, mixture toxicity, and bioconcentration factors. Furthermore, we compared these prediction values for aquatic toxicity with experimental results to evaluate the models' accuracy.

3.3.1. Baseline toxicity and Toxic Ratio

Among the oxo-LOHC compounds, the hydrophobicity generally increases as one progresses from the H_2-lean (aromatic) form to the H_2-rich form (aliphatic) within each system. For neutral organic compounds, the log K_{OW} value is a good indicator of the affinity to lipids and can be used to estimate the aquatic toxicity as the correlation between the toxicity and hydrophobicity of such compounds is well established [52]. The log K_{OW} values for oxo-LOHC compounds in this study range from 1.58 to 4.68 (Table 1) and, as expected, are lower for the H0-ACP and H8-ACP (log K_{OW} 1.58 and 2.24) than for the oxo-LOHC compounds with two rings (log K_{OW} ranging from 2.67 to 4.68). The toxicity based on the hydrophobicity-driven partitioning into biological membranes is the minimum level of toxicity that a compound can exhibit, and is therefore termed the "baseline toxicity". Indeed, we found that EC_{50} values for oxo-LOHC compounds were inversely correlated with the log K_{OW} values (Table 1, Fig. 3), which is a prerequisite of baseline toxicity. In other words, as the log K_{OW} value increases, the EC_{50} value decreases and toxicity rises (Fig. 3).

The initial QSAR models applied in screening-level hazard assessment assume that compounds are baseline toxicants and use log K_{OW} (or log K_{MW}) to predict toxicity. Excess toxicity is toxicity caused by the compound under test conditions reacting or interacting with specific biomolecules (e.g. receptors, enzymes, and DNA) and usually occurs at lower concentrations. Therefore, using models designed to predict baseline toxicity for compounds that also exhibit excess toxicity would result in an underestimation of toxicity. The baseline QSAR models are therefore helpful to be able to, at least, distinguish if the tested LOHC compounds are baseline or excess toxicants.

We applied baseline toxicity models for three test species to LOHC compounds and compared experimental results to model predictions (Fig. 3, A-C). To classify oxo-LOHC compounds, we adopted the Toxic Ratio concept (TR; Eq. 5) introduced by Verhaar et al. [52] that serves as a tool for classifying compounds into baseline (narcotic), or excess toxicants by employing a baseline toxicity QSAR model:

$$Toxic\ Ratio = \frac{EC_{50,baseline}}{EC_{50,experiment}} \quad (5)$$

$EC_{50,baseline}$ denotes the predicted value obtained from a baseline toxicity QSAR model based on the relationship between log K_{OW} and EC_{50} (Fig. 3. A–C), while $EC_{50,experiment}$ is obtained from the laboratory experiments.

Fig. 3. (D) shows that the TR values for oxo-LOHC compounds fall in the range of 0.1 ~ 10 indicating that oxo-LOHC compounds can be considered as baseline toxicants for the three tested aquatic organisms [53–55]. Likewise, most oxo-LOHC compounds distribute within a range of one order of magnitude from the respective QSAR (Fig. 3. A-C). As outliers, H0–3-MBP exhibited a TR value of 29 in the *R. subacapitata* test, corresponding to excess toxicity, whereas the TR value for H0–4-MBP in the *R. subcapitata* test and H0-ACP in the *A. fischeri* test are only slightly above the threshold value of 10. The position of a methyl group seems to play a role in determining algal toxicity since H0–3-MBP exhibits clear excess toxicity while other isomers do not. In contrast to the ortho position, the presence of a methyl group at the meta or, to a lesser extent, the para position in methylbenzophenones might lead to the excess toxicity exhibited against *R. subcapitata*. This could be attributed to the so-called 'methyl effect' observed for some drugs, where the presence of a methyl group enhances the binding affinity for active sites [56]. Similar significant differences in toxicity, due to changing the position of the methyl group, were also observed for 1,2-dimethyl-naphthalene and 1,3-dimethyl-naphthalene in the literature [57]. The EC_{50} of the former against *R. subcapitata* is 4.2 mg/L, while the latter has an EC_{50} of 0.62 mg/L, approximately 7 times lower. Except for two methylbenzophenones, the Toxic Ratio of oxo-LOHC compounds suggests that their acute toxic effect is mainly driven by the hydrophobicity and does not induce a specific mode of toxic action to the three tested organisms [52].

3.3.2. Determination of the log K_{MW} and comparison with prediction models

In the case of baseline toxicity, hydrophobic compounds intercalate into lipid membranes and disrupt their integrity [58]. In this regard, lipid-membrane partition coefficients (log K_{MW}), rather than log K_{OW} values (derived from a bulk solvent, octanol), can better represent the interaction of some compounds with the membrane [59] and its concomitant toxicity. To examine whether this holds true for oxo-LOHC compounds, we measured their log K_{MW} using solid supported liquid membranes (SSLM) composed of phosphatidylcholine (POPC,

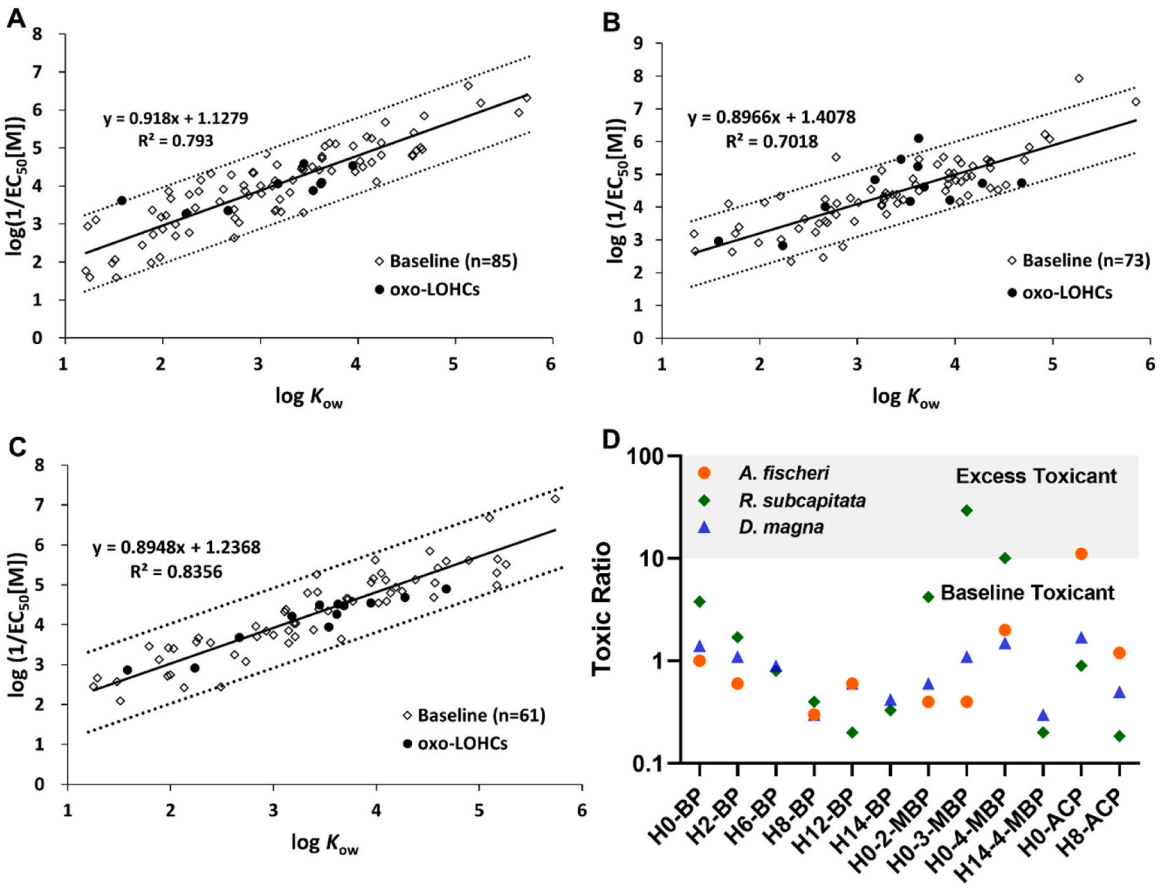

Fig. 3. Three QSAR models for baseline toxicity: (A) *A. fischeri* from Ref. [53], (B) *R. subcapitata* from Ref. [54], and (C) *D. magna* from Ref. [55]. White diamonds are known baseline toxicants, while black circles represent oxo-LOHC compounds. Solid line represents the respective QSAR and dotted lines indicate one order of magnitude from the trend line of baseline toxicants. See Text S2 for the detailed information about QSAR models. (D) Toxic Ratio of oxo-LOHCs in three acute toxicity tests.

TRANSIL^{TM}). The measurement of K_{MW} using SSLMs is relatively costly and has its limits (e.g. log K_{MW} values lower than 1.5 or higher than 5.5 cannot be measured) [60] which did not allow for the experimental determination of K_{MW} of the H0-ACP/H8-ACP system.

We found that empirical log K_{MW} values range from 2.88 to 3.91 in a similar range of log K_{OW} values (Table 1). A somewhat higher difference between log K_{OW} and log K_{MW} can be observed for the H_2-rich forms of the carriers (H14-BP and H14–4-MBP). Nevertheless, log K_{OW} and log K_{MW} correlate well for oxo-LOHC compounds (Fig. S6; R^2 =0.8693). Such a good agreement of both parameters was previously observed for neutral organic compounds [61,62]. Thus, log K_{OW} was used as a parameter for the baseline toxicity in this study. Additionally, we used *in silico* models to estimate log K_{MW} and aimed to assess their general applicability for oxo-LOHCs. First model was COSMOmic that predicts partitioning of oxo-LOHCs into POPC by treating the bilayer structure of POPC as anisotropic, layered structure. The predicted log K_{MW} values for seven compounds (H0-BP, H2-BP, H6-BP, H8-BP, H0–2-MBP, H0–3-MBP, and H0–4-MBP) were found to be in very close agreement with the experimental values. However, the log K_{MW} values for three hydrogenated forms (H12-BP, H14-BP, and H14–4-MBP) were over-predicted by more than one order of magnitude (compared to experimental values; Fig. 4). This overprediction may be attributed to COSMOmic considering only the direct interactions between surface fragments of the solute and the lipid membrane, while neglecting their 3D structure and resulting steric effects. Secondly, we used the poly-parameter linear free energy relationship (pp-LFER) model developed by Endo and coworkers [61] to predict log K_{MW} values. The pp-LFER model is robust and accurate when used to predict log K_{MW} for

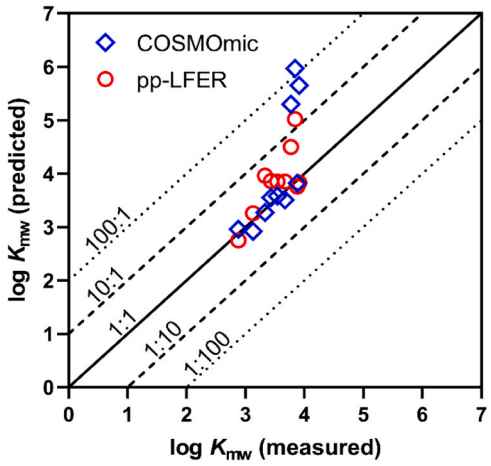

Fig. 4. Comparison of the predicted and measured values of membrane-water partition coefficients (log K_{MW}). Predictions were performed using COSMOmic at TZVPD-FINE (blue diamond) and pp-LFER (red circle).

various chemical classes - due to the fact that it incorporates descriptors of polar and nonspecific interactions, i.e. hydrogen bond, polarizability, and van der Waals interaction. The accuracy of prediction was within 0.08 to 1.17 log units. As with COSMOmic, the predicted values for hydrogenated forms deviate the most from the experimental values, by 0.73 for H14-BP and 1.17 for H14–4-MBP (Fig. 4). The overpredictions

by both models may be attributed to the limited number of compounds with multiple cyclic aliphatic moieties in the training set of the software [24,30,61,63,64]. However, the reason for this deviation cannot be clarified with certainty. In general, both models provide reliable estimates for log K_{MW} of aromatic oxo-LOHC compounds [30,61]. Detailed information on the descriptors can be found in Table S7.

3.3.3. Estimated mixture toxicity of the benzophenone-based LOHC system

LOHC systems in practical use are typically mixtures of technical grade products. As neither the LOHC hydrogenation (to charge the system) nor the LOHC dehydrogenation (to uncharge) are quantitative conversion steps, there are usually mixtures of compounds with different degrees of hydrogenation/dehydrogenation present in an LOHC system. In addition, small quantities of high or low boiling side products have been found under laboratory conditions [8]. Diphenylmethane, the deoxygenated product of benzophenone, and its hydrogenated forms are also observed in the BP-based carrier system due to some hydrodeoxygenation activity of the applied catalytic system [8]. Note, that in some application cases, dehydrogenation is intentionally limited to less than 100 % or other carriers or even solvents are mixed with the original oxo-LOHC system in order to keep the carrier system liquid under storage conditions [65–67].

To start addressing the issue of mixture toxicity, we evaluated mixtures of six-LOHC compounds in the H0-BP/H14-BP LOHC system, using *D. magna*. Given that these LOHC compounds have been found to be baseline toxicants in acute tests with *D. magna*, we used the concentration addition (CA) model. The CA model is applicable when the components of a mixture share "a common site of action" [32], here the cell membrane. According to the CA model, the effective concentration of the mixture can be calculated based on the known effective concentrations of the components (tested individually) forming the mixture. We prepared a mixture of six components of the H0-BP/H14-BP system by mixing them in quantities proportional to the toxicity of each individual compound. The experimentally determined EC_{50} of the mixture was 18.7 (18.4–19.2) mg/L and, thus, was close to the theoretical EC_{50} predicted using the CA model (14.5 mg/L). Fig. 5 shows that below 80 % immobilization the effect of the mixture was lower than predicted by the CA model. Beyond 80 %, the experimental results were in close agreement with the CA prediction. The index of prediction quality of the CA model (IPQ_{CA}; Eq. 2) is 0.298, indicating a good agreement between the CA model and the experimental result as the IPQ_{CA} is close to zero. On the other hand, the IA model underestimates the toxicity of the mixture as it yields approximately 40 % immobilization at the highest tested concentration (24.7 mg/L). Thus, the CA model predicts the effect of mixtures well for our test system (*D. magna*) and allows an effective preliminary assessment of LOHC mixtures as long as the individual compounds are baseline toxicants.

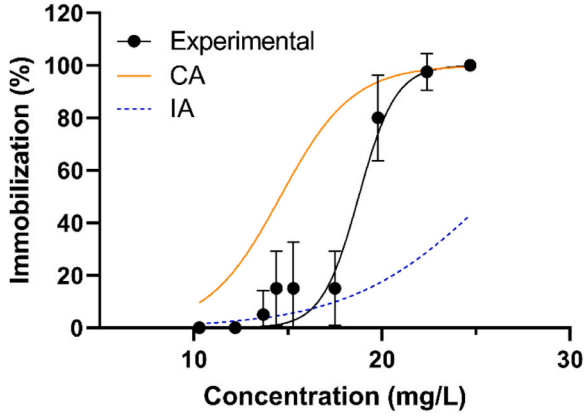

Fig. 5. The concentration-response curve of the mixture toxicity test (*D. magna*). The orange line represents the concentration addition (CA) model and blue dashed line represents the independent action (IA) model. Black circles represent the experimental results from this study. Error bars represent the standard deviation.

3.3.4. Estimated bioconcentration factors and bioaccumulation potential

Assessing the bioaccumulation potential of a chemical is an important aspect of a hazard assessment. Bioaccumulation is the enrichment of chemicals in organisms, relative to the concentration present in the surrounding environment. Bioaccumulation potential is most often assessed using fish bioaccumulation tests and compounds are considered bioaccumulative if the ratio of concentration in fish, relative to the exposure medium, is higher than 2000 (log BCF = 3.3) [68]. Given the constraints of cost and animal welfare, computational models have gained widespread usage for a preliminary assessment of bioaccumulation. In this regard, two models were used in this study to estimate the bioconcentration factor of oxo-LOHC compounds. One model developed by Dołżonek et al. (Eq. (6)) [69] is based on a correlation between empirical log K_{MW} [61] and the bioconcentration factor (BCF) [70] for organic compounds. The membrane-water partition coefficient is a biologically relevant parameter for the estimation of the bioaccumulation potential of chemicals which interact with biological membranes rather than storage lipids [61].

$$\log BCF = 0{\cdot}80 \log K_{MW} - 0{\cdot}95 \quad (6)$$

Secondly, the Arnot-Gobas model was employed. The Arnot-Gobas model uses uptake (through respiration, dietary ingestion, and dermal absorption) and elimination (through respiration, faecal egestion, and metabolic transformation) rates to calculate bioaccumulation factors [71]. The model requires log K_{OW} as an input parameter and generates predictions of bioaccumulation factors for three trophic levels of fish species. In this study, BCF values for the upper trophic level were used for the analysis because these upper trophic species represent the worst-case scenario.

The log K_{MW}-based model proposed by Dołżonek et al. estimated the BCF of oxo-LOHC compounds to be in the range of 1.08 to 150, while the log K_{OW}-based model of Arnot and Gobas yielded BCF values ranging from 3.93 to 653 (Table 2). These two models show good agreement, with the largest difference between the two models of 520 (or 0.7 log units) for H14–4-MBP. Based on the predicted BCF, none of the tested oxo-LOHC compounds seems to be bioaccumulative in fish – at least according to the REACH bioaccumulation criterion (BCF > 2000) [68]. According to more stringent GHS criteria (BCF >500 or log K_{OW} > 4.0) [43], H14-BP and H14–4-MBP could be potentially considered as

Table 2
Bioconcentration factors (BCFs) of oxo-LOHCs obtained using two models.

Compound	Dołżonek et al.[a] BCF	Arnot-Gobas[b] BCF
H0-BP	35.6	23.9
H2-BP	22.8	18.5
H6-BP	142	155
H8-BP	52.0	72.9
H12-BP	150	285
H14-BP	117	354
H0-2-MBP	62.7	195
H0-3-MBP	76.1	198
H0-4-MBP	96.1	152
H14-4-MBP	133	653
H0-ACP	1.08[c]	3.93
H8-ACP	5.58[c]	14.8

[a] QSAR model from Ref. [69] was developed using the correlation between log K_{MW} and log BCF.

[b] BCFBAF v 3.01 is based on the Arnot-Gobas model [71] - a single parameter QSAR using log K_{OW}. Estimated log K_{OW} values (KOWWIN v1.68) were used as input for the model when no experimental values were available.

[c] For H0-ACP and H8-ACP, COSMOmic (TZVPD-FINE)-predicted log K_{MW} values were used to derive BCFs.

bioaccumlative (Table 2). Since both BCF and log K_{OW} values of the two compounds are estimated values, this assessment should be considered as preliminary.

3.4. Endocrine activity of oxo-LOHC compounds using yeast-based reporter gene assays

The effect of oxo-LOHC compounds on endocrine activity was investigated using four yeast-based reporter gene assays, designed to detect interactions with the human estrogen receptor alpha (hERα) in YES and YAES tests, and the human androgen receptor (hAR) in YAS and YAAS tests. Both agonistic (binding to the receptor and eliciting response) and antagonistic (blocking the receptor without eliciting response) effects were investigated. The observed effects were compared with dose-response curves of respective positive controls (17β-estradiol (E2), testosterone (T), 4-hydroxytamoxifen (OHT), and flutamide (FLU)) (Fig. S2) and then bioanalytical equivalents were calculated (Fig. 6). The test concentration, 2 mg/L (ca. 10^{-5} M), was selected because benzophenone and its derivatives exhibited estrogen or androgen receptor-mediated effects at this concentration [20,22,23]. In addition, 4-hydroxybenzophenone (4-OH-BP) was included in Fig. 6 for a comparison at 2 mg/L because 4-OH-BP showed estrogenic and androgenic activity in the literature [23].

3.4.1. Estrogenic and antiestrogenic activities

The estrogenic (YES assay) and anti-estrogenic (YAES assay) effects of the oxo-LOHC compounds tested at 2 mg/L were below the assay's LOQ, while 4-OH-BP showed a low level of positive response in the YES test, but not in the YAES test (< LOQ) [23]. The structural feature of 17β-estradiol (E2; a sex hormone) known to be responsible for its estrogenic potential is the hydroxyl group at the third position of the A-ring. This hydroxyl group plays a crucial role in hydrogen binding to the estrogen receptor's (ER's) ligand-binding domain [72]. Additionally, the hydrophobic backbone (containing at least one aromatic ring) and another hydrogen bond donor (like a hydroxyl group in the D-ring of the E2) are necessary for binding [72]. Due to possessing such structural features, the hydroxylated benzophenones exhibited estrogenic activity in yeast screen assays, presumably by making direct hydrogen bonds with the ER [22,23,73] as the OH-BP's hydroxyl group is similarly positioned to the hydroxyl group of the A-ring of E2 [74]. Hence, it can be deduced that benzophenone and methylbenzophenones, which lack a hydroxyl group at position 4 of the phenyl ring, are unable to form a hydrogen bond with the ER. This observation reaffirms the argument that the estrogenic potential of benzophenone is eliminated, when the hydroxyl group on the phenyl ring is missing [75]. The same principles may be extended to the rest of the oxo-LOHC compounds - a hydroxyl group in the middle of the structure (H2-BP, H8-BP, H14-BP, and H14–4-MBP) does not seem to be able to make a hydrogen bond with the ER. Additionally, the absence of the aromatic ring in aliphatic oxo-LOHC compounds (H12-BP, H14-BP, and H14–4-MBP) may lead to a lack of potency as the ER ligand-binding domain requires the presence of an aromatic ring [72]. Steroids without an aromatic ring have shown weak binding affinity in previous studies, despite their conformational similarity to E2 [76,77].

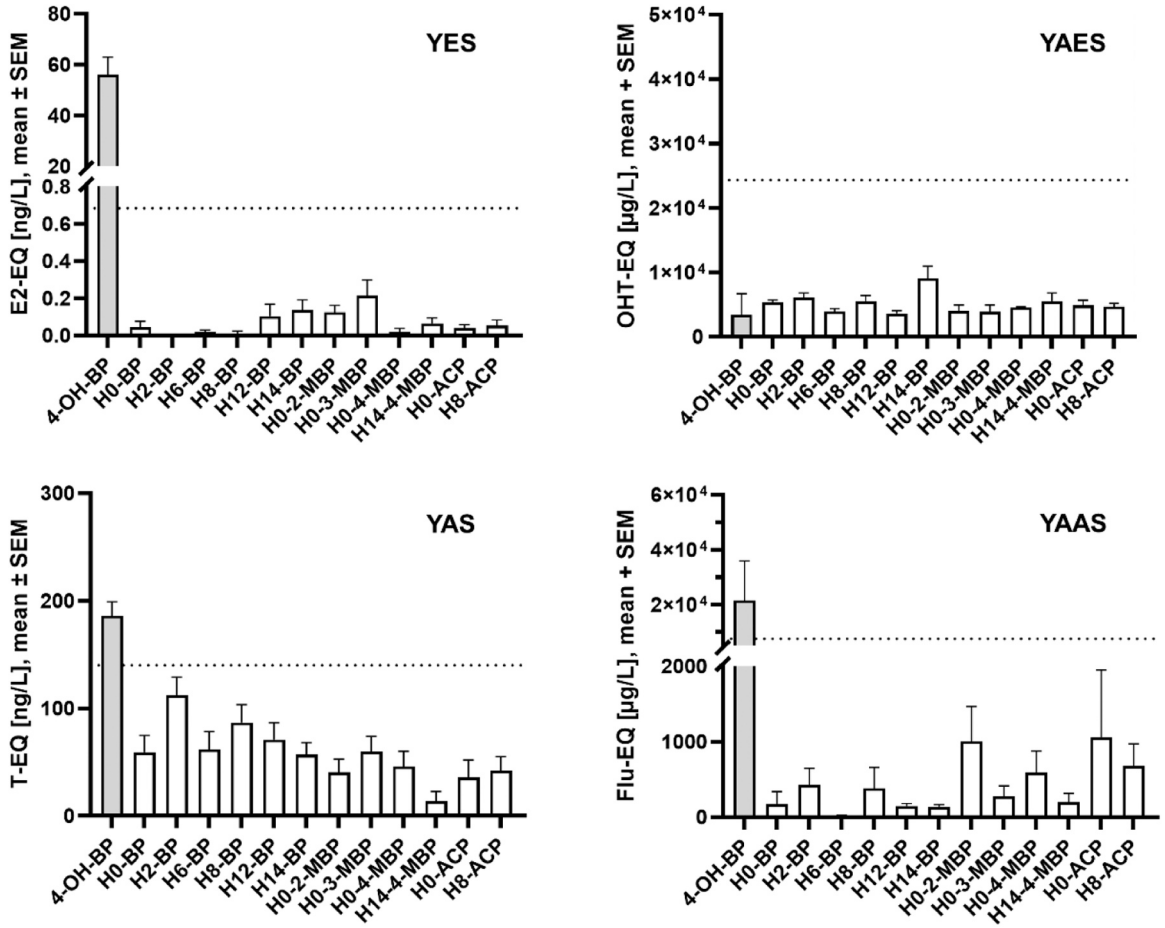

Fig. 6. Endocrine activity of oxo-LOHC compounds shown as bioanalytical equivalents of: 17β-estradiol equivalents (E2-EQ) in YES, 4-hydroxytamoxifen-equivalents (OHT-EQ) in YAES, testosterone equivalents (T-EQ) in YAS, and flutamide-equivalents (FLU-EQ) in YAAS. Data are shown as mean values from one experiment (n = 8). Error bars represent standard error of the mean (SEM). The dotted lines indicate the LOQ of each assay. 4-hydroxybenzophenone (4-OH-BP) data were taken from Carstensen et al. [23].

3.4.2. Androgenic and antiandrogenic activities

The androgenic and anti-androgenic effects of oxo-LOHCs tested at 2 mg/L were below the assay's LOQ, while 4-OH-BP exhibited a response higher than the LOQ in YAS, and YAAS tests [23]. The structural features of dihydrotestosterone that are important for binding to the androgen receptor are: the ketone group on the A-ring (3-position) and the hydroxyl group on the D-ring (17-position) [78]. The positions of these two functional groups are the same as two hydroxyl groups in 17β-estradiol (E2). Similar to how 4-OH-BP functions as an ER ligand, 4-OH-BP seems to act as an AR ligand by hydrogen bonding with an arginine or asparagine/threonine residue where testosterone also forms hydrogen bonds [78]. Although all oxo-LOHC compounds have a ketone group or hydroxyl group in their structure that could be either a hydrogen donor or acceptor, their positions do not seem to enable a close interaction with the hAR. These structural features in oxo-LOHC compounds might be the reason for the not observable effect in this study, even though many phenols possessing only one group capable of hydrogen bonding show low but detectable binding to recombinant AR [78]. The lack of an effect observed with oxo-LOHC compounds with one ring (H0-ACP and H8-ACP) is in-line with the result of Carstensen et al. with two compounds in a mono-ring structure, 4-cresol and benzoate, that lack androgen activity in yeast screening assays [23]. The result that H0-ACP and H8-ACP do not bind to the hAR can also be attributed to their relatively low hydrophobicity - hydrophobic interactions have been found to be important for the binding of non-steroids (e.g. phenols and phytoestrogens) to the AR in the log K_{OW} range from 1 to 7 [72,78]. In a mammalian reporter gene assay (hAR), the androgenic effect of H0-BP was observed at concentrations one order of magnitude higher than tested here, and a significant anti-androgenic effect was observed with an 50 % inhibition concentration value of 14 mg/L [79]. Since the interaction of benzophenones (with both the ER and the AR) is increased upon hydroxylation, which can occur in the environment as a result of microbial degradation [23,80] or as the result of enzymatic metabolism in an organism (e.g. rat hepatocytes) [81], it is still possible that oxo-LOHCs might demonstrate endocrine activity upon metabolic activation. Additionally, non-human species may respond differently to oxo-LOHC compounds due to different sensitivity [82,83]. Therefore, the results in this study might be an underestimation of the true potency of oxo-LOHC compounds and should be regarded as a preliminary assessment.

4. Conclusions

The assessment of aquatic toxicity shows that most oxo-LOHC compounds exhibit moderate acute toxicity and fall under the "toxic" or "harmful to aquatic organisms" classification according to the GHS criteria. Furthermore, the toxic ratio of oxo-LOHC compounds indicates that their toxicity is nonspecific (baseline toxicity). This is linked to the mode of action, which is the intercalation of a compound into the membrane, resulting in impaired membrane integrity. This nonspecific effect of oxo-LOHC compounds was further supported by the concentration-additive behavior observed in the mixture toxicity test with benzophenone and its five hydrogenated forms using *D. magna*. Furthermore, yeast screening assays showed no estrogen and androgen receptor-mediated effects, supporting the nonspecific mode of toxic action. However, there is a possibility that hydroxylation of the LOHC, due to microbial or metabolic degradation, might increase the estrogenic or androgenic activity as has been observed in the case of benzophenone-based UV-filter [23,80]. Lastly, a low bioconcentration/bioaccumulation potential for oxo-LOHC compounds was estimated using partitioning coefficients as parameters in each model.

On the basis of aquatic toxicity tests and yeast screening assays, structure-activity relationships can be derived. First, across the three tested organisms, the hydrophobicity of a compound appears to be the main driver of aquatic toxicity rather than a certain structural element. Exceptions are H0–3-MBP and H0–4-MBP that showed EC_{50} values below 1 mg/L in algae toxicity test and TR values above 10. This may suggest that methyl substitution on the aromatic ring may cause excess toxicity, likely depending on the position of the methyl group, as H0–2-MBP showed comparable toxicity to H0-BP. Further research is warranted to elucidate the influence of methyl group position and the specific mode of action. Secondly, the position of hydroxyl groups on the chemical structure appears to determine estrogenic or androgenic activity. As reported in the literature, the hydroxyl group on position 3 or 4 of the ring can interact with ER and AR receptor [23,74,75], whereas a hydroxyl group positioned in the center of two-ring structures, as found in oxo-LOHC compounds, appears to be unable to make a close interaction. Overall, the H0-ACP/H8-ACP LOHC system is the most environmentally favorable among the oxo-LOHC systems investigated because of its low aquatic toxicity.

The research findings of this study, which indicate moderate ecotoxicity and low bioaccumulation potential for the tested oxo-LOHC compounds, combined with their favorable technological characteristics make them highly promising candidates for future hydrogen storage and transportation applications. Further research should investigate the behaviour of oxo-LOHCs in the environment including their mobility and especially their biodegradability, which is an important factor that influences the likelihood of other hazards occurring. In the case that the persistence of oxo-LOHC compounds is found to be considerable, it is also necessary to assess the potential for chronic toxicity. Lastly, it would be beneficial to consider the side products being formed during the (de) hydrogenation process, such as diphenylmethane in the BP-based system [8]. A comprehensive environmental hazard assessment will ensure that we are well prepared to address all issues related to the newly implemented and highly anticipated LOHC systems. It will enable us to be confident that we have truly found a "clean technology" with which to power the future.

Environmental implications

The potential widespread use of LOHC systems as a replacement for fossil fuels comes with the concern, that large quantities of organic compounds may reach the environment in the event of an accident. To address this concern, this study provides data on aquatic toxicity, bioaccumulation potential, and human estrogen/androgen activity for three oxo-LOHC systems. This study contributes to our understanding of the environmental impact of oxo-LOHC systems, supports LOHC developers and regulatory agencies in making informed decisions regarding the safe implementation of oxo-LOHC systems, and facilitates the choice of the most suitable LOHC system from growing portfolio of potential carriers.

CRediT authorship contribution statement

Yohan Seol: Writing – original draft, Investigation, Data curation. **Marta Markiewicz:** Writing – review & editing, Investigation, Conceptualization. **Stephan Beil:** Writing – review & editing, Validation, Data curation. **Sara Schubert:** Writing – review & editing. **Dirk Jungmann:** Writing – review & editing. **Peter Wasserscheid:** Writing – review & editing, Conceptualization. **Stefan Stolte:** Writing – review & editing, Supervision, Resources, Investigation, Conceptualization.

Declaration of Competing Interest

The authors declare the following financial interests/personal relationships which may be considered as potential competing interests: Peter Wasserscheid reports a relationship with Hydrogenious LOHC Technologies GmbH that includes: equity or stocks. If there are other authors, they declare that they have no known competing financial interests or personal relationships that could have appeared to influence the work reported in this paper.

Data availability

Data will be made available on request.

Acknowledgement

This research is supported by the Kurt Eberhard Bode Stiftung and Deutsches Stiftungszentrum with a grant T 0122/33742/2019/kg as well as by Saxon State Ministry of Science and Art (SMWK). Additionally, Yohan Seol was supported by the Saxon scholarship program. We thank René Zippel for his experimental support in yeast reporter gene assays and Dr. Viktor Schmalz for the development of analytical method.

Appendix A. Supporting information

Supplementary data associated with this article can be found in the online version at doi:10.1016/j.jhazmat.2024.135102.

References

[1] Preuster, P., Papp, C., Wasserscheid, P., 2017. Liquid Organic Hydrogen Carriers (LOHCs): toward a hydrogen-free hydrogen economy. Acc Chem Res 50, 74–85. https://doi.org/10.1021/acs.accounts.6b00474.
[2] Züttel, A., Remhof, A., Borgschulte, A., Friedrichs, O., 2010. Hydrogen: the future energy carrier. Philos Trans A Math Phys Eng Sci 368, 3329–3342. https://doi.org/10.1098/rsta.2010.0113.
[3] Rüde, T., Dürr, S., Preuster, P., Wolf, M., Wasserscheid, P., 2022. Benzyltoluene/perhydro benzyltoluene – pushing the performance limits of pure hydrocarbon liquid organic hydrogen carrier (LOHC) systems. Sustain Energy Fuels. https://doi.org/10.1039/d1se01767e.
[4] Preuster, P., Alekseev, A., Wasserscheid, P., 2017. Hydrogen storage technologies for future energy systems. Annu Rev Chem Biomol Eng 8, 445–471. https://doi.org/10.1146/annurev-chembioeng-060816-101334.
[5] Chiyoda Corporation, Chiyoda Corporation sign an MOU to study importing hydrogen on a commercial scale into the Port of Rotterdam, The Netherlands, using SPERA Hydrogen™; 2021. https://www.chiyodacorp.com/media/20210730_E.pdf (Accessed 1 January 2022).
[6] Hydrogenious LOHC Technologies GmbH, Worldwide novelty: Hydrogenious supplies hydrogen filling station in Erlangen/Germany via Liquid Organic Hydrogen Carriers; 2022. https://www.linkedin.com/company/hydrogenious-lohc/posts/?feedView=all [accessed 25 July 2022].
[7] Hydrogenious GmbH, Novel path towards safe zero-emission shipping: Hydrogenious LOHC Technologies and Østensjø Group join forces with tailwind from Enova funding; 2021.
[8] Zakgeym, D., Hofmann, J.D., Maurer, L.A., Auer, F., Müller, K., Wolf, M., et al., 2023. Better through oxygen functionality? The benzophenone/dicyclohexylmethanol LOHC-system. Sustain Energy Fuels 7, 1213–1222. https://doi.org/10.1039/d2se01750d.
[9] Sievi, G., Geburtig, D., Skeledzic, T., Bösmann, A., Preuster, P., Brummel, O., et al., 2019. Towards an efficient liquid organic hydrogen carrier fuel cell concept. Energy Environ Sci 12, 2305–2314. https://doi.org/10.1039/c9ee01324e.
[10] Zhang, C., Liang, X., Liu, S., 2011. Hydrogen production by catalytic dehydrogenation of methylcyclohexane over Pt catalysts supported on pyrolytic waste tire char. Int J Hydrogen Energy 36, 8902–8907. https://doi.org/10.1016/j.ijhydene.2011.04.175.
[11] Boufaden, N., Akkari, R., Pawelec, B., Fierro, J.L.G., Zina, M.S., Ghorbel, A., 2016. Dehydrogenation of methylcyclohexane to toluene over partially reduced silica-supported Pt-Mo catalysts. J Mol Catal A Chem 420, 96–106. https://doi.org/10.1016/j.molcata.2016.04.011.
[12] European Union, Chemicals strategy - European Commission; 2020. https://environment.ec.europa.eu/strategy/chemicals-strategy_en (Accessed 8 April 2024).
[13] Markiewicz, M., Zhang, Y., Bösmann, A., Brückner, N., Thöming, J., Wasserscheid, P., et al., 2015. Environmental and health impact assessment of liquid organic hydrogen carrier (LOHC) systems - challenges and preliminary results. Energy Environ Sci 8, 1035–1045.
[14] Zhang, Y.-Q., Markiewicz, M., Filser, J., Stolte, S., 2018. Toxicity of a quinaldine-based liquid organic hydrogen carrier (LOHC) system toward soil organisms Arthrobacter globiformis and Folsomia candida. Environ Sci Technol 52, 258–265. https://doi.org/10.1021/acs.est.7b04434.
[15] Markiewicz, M., Zhang, Y.-Q., Empl, M.T., Lykaki, M., Thöming, J., Steinberg, P., et al., 2019. Hazard assessment of quinaldine-, alkylcarbazole-, benzene- and toluene-based liquid organic hydrogen carrier (LOHCs) systems. Energy Environ Sci 12, 366–383. https://doi.org/10.1039/C8EE01696H.
[16] Zhang, Y.Q., Stolte, S., Alptekin, G., Rother, A., Diedenhofen, M., Filser, J., et al., 2020. Mobility and adsorption of liquid organic hydrogen carriers (LOHCs) in soils-environmental hazard perspective. Green Chem 22, 6519–6530. https://doi.org/10.1039/d0gc02603d.
[17] Schug, T.T., Johnson, A.F., Birnbaum, L.S., Colborn, T., Guillette, L.J., Crews, D.P., et al., 2016. Minireview: endocrine disruptors: past lessons and future directions. Mol Endocrinol 30, 833–847. https://doi.org/10.1210/me.2016-1096.
[18] Molins-Delgado, D., Gago-Ferrero, P., Díaz-Cruz, M.S., Barceló, D., 2016. Single and joint ecotoxicity data estimation of organic UV filters and nanomaterials toward selected aquatic organisms. Urban groundwater risk assessment. Environ Res 145, 126–134. https://doi.org/10.1016/j.envres.2015.11.026.
[19] Liu, H., Sun, P., Liu, H., Yang, S., Wang, L., Wang, Z., 2015. Acute toxicity of benzophenone-type UV filters for Photobacterium phosphoreum and Daphnia magna: QSAR analysis, interspecies relationship and integrated assessment. Chemosphere 135, 182–188. https://doi.org/10.1016/j.chemosphere.2015.04.036.
[20] Zhang, Q., Ma, X., Dzakpasu, M., Wang, X.C., 2017. Evaluation of ecotoxicological effects of benzophenone UV filters: Luminescent bacteria toxicity, genotoxicity and hormonal activity. Ecotoxicol Environ Saf 142, 338–347. https://doi.org/10.1016/j.ecoenv.2017.04.027.
[21] Nendza, M., Wenzel, A., Müller, M., Lewin, G., Simetska, N., Stock, F., et al., 2016. Screening for potential endocrine disruptors in fish: evidence from structural alerts and in vitro and in vivo toxicological assays. Environ Sci Eur 28, 26. https://doi.org/10.1186/s12302-016-0094-5.
[22] Kunz, P.Y., Fent, K., 2006. Estrogenic activity of UV filter mixtures. Toxicol Appl Pharmacol 217, 86–99. https://doi.org/10.1016/j.taap.2006.07.014.
[23] Carstensen, L., Zippel, R., Fiskal, R., Börnick, H., Schmalz, V., Schubert, S., et al., 2023. Trace analysis of benzophenone-type UV filters in water and their effects on human estrogen and androgen receptors. J Hazard Mater 456. https://doi.org/10.1016/j.jhazmat.2023.131617.
[24] Loidl-Stahlhofen, A., Hartmann, T., Schöttner, M., Rhöring, C., Brodowsky, H., Schmitt, J., et al., 2001. Multilamellar liposomes and solid-supported lipid membranes (TRANSIL): screening of lipid-water partitioning toward a high-throughput scale. Pharm Res 18, 1782–1788. https://doi.org/10.1023/A:1013343117979.
[25] COSMOlogic GmbH & Co.K.G., COSMOtherm, Version C30, Release 18; 2018. http://www.cosmologic.de (Accessed 10 November 2023).
[26] Eckert, F., Klamt, A., 2002. Fast solvent screening via quantum chemistry: COSMO-RS approach. AIChE J 48, 369–385. https://doi.org/10.1002/aic.690480220.
[27] TURBOMOLE GmbH, TURBOMOLE V7.3 2018, a development of University of Karlsruhe and Forschungszentrum Karlsruhe GmbH, 1989–2007, TURBOMOLE GmbH, since 2007, (2018). http://www.turbomole.com (Accessed 10 November 2023).
[28] Schäfer, A., Huber, C., Ahlrichs, R., 1994. Fully optimized contracted Gaussian basis sets of triple zeta valence quality for atoms Li to Kr. J Chem Phys 100, 5829–5835. https://doi.org/10.1063/1.467146.
[29] Klamt, A., Diedenhofen, M., 2018. A refined cavity construction algorithm for the conductor-like screening model. J Comput Chem 39, 1648–1655. https://doi.org/10.1002/jcc.25342.
[30] Klamt, A., Huniar, U., Spycher, S., Keldenich, J., 2008. COSMOmic: a mechanistic approach to the calculation of membrane−water partition coefficients and internal distributions within membranes and micelles. J Phys Chem B 112, 12148–12157. https://doi.org/10.1021/jp801736k.
[31] Jakobtorweihen, S., Ingram, T., Smirnova, I., 2013. Combination of COSMOmic and molecular dynamics simulations for the calculation of membrane-water partition coefficients. J Comput Chem 34, 1332–1340. https://doi.org/10.1002/jcc.23262.
[32] Altenburger, R., Backhaus, T., Boedeker, W., Faust, M., Scholze, M., Grimme, L.H., 2000. Predictability of the toxicity of multiple chemical mixtures to Vibrio fischeri: mixtures composed of similarly acting chemicals. Environ Toxicol Chem 19, 2341–2347. https://doi.org/10.1002/etc.5620190926.
[33] Altenburger, R., Boedeker, W., Faust, M., Grimme, L.H., 1996. Regulations for combined effects of pollutants: Consequences from risk assessment in aquatic toxicology. Food Chem Toxicol 34, 1155–1157. https://doi.org/10.1016/S0278-6915(97)00088-4.
[34] Escher, B.I., Van Daele, C., Dutt, M., Tang, J.Y.M., Altenburger, R., 2013. Most oxidative stress response in water samples comes from unknown chemicals: the need for effect-based water quality trigger values. Environ Sci Technol 47, 7002–7011. https://doi.org/10.1021/es304793h.
[35] C. Hansch, A. Leo, D.H. Hoekman, Exploring QSAR: Hydrophobic, Electronic, and Steric Constants, American Chemical Society, Washington, DC, 1995. https://pubs-acs-org.proxy.library.uu.nl/doi/full/10.1021/jm950902o.
[36] Kusk, K.O., Christensen, A.M., Nyholm, N., 2018. Algal growth inhibition test results of 425 organic chemical substances. Chemosphere 204, 405–412. https://doi.org/10.1016/j.chemosphere.2018.04.047.
[37] Pawlisz, A.V., Peters, R.H., 1993. A radioactive tracer technique for the study of lethal body burdens of narcotic organic chemicals in Daphnia magna. Environ Sci Technol 27, 2795–2800. https://doi.org/10.1021/es00049a019.
[38] Pawlisz, A.V., Peters, R.H., 1995. Effects of sublethal exposure on lethal body burdens of narcotic organic chemicals in Daphnia magna. Environ Sci Technol 29, 613–621. https://doi.org/10.1021/es00003a008.
[39] Galassi, S., Mingazzini, M., Viganò, L., Cesareo, D., Tosato, M.L., 1988. Approaches to modeling toxic responses of aquatic organisms to aromatic hydrocarbons. Ecotoxicol Environ Saf 16, 158–169. https://doi.org/10.1016/0147-6513(88)90030-9.
[40] Bobra, A.M., Shin, W.Y., Mackay, D., 1983. A predictive correlation for the acute toxicity of hydrocarbons and chlorinated hydrocarbons to the water flea (Daphniamagna). Chemosphere 12, 1121–1129. https://doi.org/10.1016/0045-6535(83)90118-2.

[41] Janssen, C.R., Persoone, G., 1993. Rapid toxicity screening tests for aquatic biota 1. Methodology and experiments with Daphnia magna. Environ Toxicol Chem 12, 711–717. https://doi.org/10.1002/etc.5620120413.
[42] Finnish Safty and Chemicals Agency, Substance Evaluation Conclusion as required by REACH Article 48 and Evaluation Report for Methylcyclohexane, Finnish Safty and Chemicals Agency, Helsinki; 2017.
[43] United Nations, GLOBALLY HARMONIZED SYSTEM OF CLASSIFICATION AND LABELLING OF CHEMICALS (GHS): Ninth revised edition, United Nations, New York and Geneva; 2021. https://unece.org/sites/default/files/2021–09/GHS_Rev9E_0.pdf.
[44] European Chemicals Agency, Benzophenone - Registration Dossier - ECHA, (n.d.). https://echa.europa.eu/registration-dossier/-/registered-dossier/13823/6/2/6 (Accessed 21 June 2023).
[45] Chiyoda Corporation, ENEOS, Chiyoda, and QUT Successfully Scaled Up an Australian CO 2 -Free Hydrogen Supply Chain Demonstration using Direct MCH ® ~ Filling a FCV with hydrogen derived from renewable energy; 2021.
[46] Chiyoda Corporation, Hydrogen Transportation in the form of MCH by Chemical Tanker; 2022. https://www.chiyodacorp.com/en/service/spera-hydrogen/innovations/ (Accessed 10 November 2023).
[47] Yamaguchi, R., Ikeda, C., Takahashi, Y., Fujita, K.I., 2009. Homogeneous catalytic system for reversible dehydrogenation-hydrogenation reactions of nitrogen heterocycles with reversible interconversion of catalytic species. J Am Chem Soc 131, 8410–8412. https://doi.org/10.1021/ja9022623.
[48] European Chemicals Agency (ECHA), Guidance on information requirements and chemical safety assessment. Chapter R.11: PBT/vPvB assessment; 2023. https://doi.org/10.2823/312974.
[49] Hale, S.E., Neumann, M., Schliebner, I., Schulze, J., Averbeck, F.S., Castell-Exner, C., et al., 2022. Getting in control of persistent, mobile and toxic (PMT) and very persistent and very mobile (vPvM) substances to protect water resources: strategies from diverse perspectives. Environ Sci Eur 34. https://doi.org/10.1186/s12302-022-00604-4.
[50] Persson, L., Carney Almroth, B.M., Collins, C.D., Cornell, S., de Wit, C.A., Diamond, M.L., et al., 2022. Outside the safe operating space of the planetary boundary for novel entities. Environ Sci Technol 56, 1510–1521. https://doi.org/10.1021/acs.est.1c04158.
[51] Escher, B.I., Altenburger, R., Blüher, M., Colbourne, J.K., Ebinghaus, R., 2023. Mod persistence – bioaccumulation – Toxic (PBT) Assess High Throughput Anim - Free Methods Subst Very High Concern 1267–1283.
[52] Verhaar, H., Van Leeuwen, C., Hermans, J., 1992. Classifying environmental pollutants. Chemosphere 25, 471–491. https://doi.org/10.1016/0045-6535(92)90280-5.
[53] Wang, X.H., Yu, Y., Huang, T., Qin, W.C., Su, L.M., Zhao, Y.H., 2016. Comparison of toxicities to Vibrio fischeri and fish based on discrimination of excess toxicity from baseline level. PLoS One 11, 1–17. https://doi.org/10.1371/journal.pone.0150028.
[54] Furuhama, A., Hasunuma, K., Hayashi, T.I., Tatarazako, N., 2016. Predicting algal growth inhibition toxicity: three-step strategy using structural and physicochemical properties. SAR QSAR Environ Res 27, 343–362. https://doi.org/10.1080/1062936X.2016.1174151.
[55] Li, J.J., Wang, X.H., Wang, Y., Wen, Y., Qin, W.C., Su, L.M., et al., 2015. Discrimination of excess toxicity from narcotic effect: Influence of species sensitivity and bioconcentration on the classification of modes of action. Chemosphere 120, 660–673. https://doi.org/10.1016/j.chemosphere.2014.10.013.
[56] Schönherr, H., Cernak, T., 2013. Profound methyl effects in drug discovery and a call for new C-H methylation reactions. Angew Chem - Int Ed 52, 12256–12267. https://doi.org/10.1002/anie.201303207.
[57] J.M. of Environment, Results of Eco-toxicity tests of chemicals conducted by Ministry of the Environment in Japan (- March 2011), (2023). https://www.env.go.jp/content/000131969.pdf (accessed November 7, 2023).
[58] Escher, B.I., Schwarzenbach, R.P., 2002. Mechanistic studies on baseline toxicity and uncoupling of organic compounds as a basis for modeling effective membrane concentrations in aquatic organisms. Aquat Sci 64, 20–35. https://doi.org/10.1007/s00027-002-8052-2.
[59] Escher, B.I., Baumer, A., Bittermann, K., Henneberger, L., König, M., Kühnert, C., et al., 2017. General baseline toxicity QSAR for nonpolar, polar and ionisable chemicals and their mixtures in the bioluminescence inhibition assay with Aliivibrio fischeri. Environ Sci Process Impacts 19, 414–428. https://doi.org/10.1039/c6em00692b.
[60] Timmer, N., Droge, S.T.J., 2017. Sorption of cationic surfactants to artificial cell membranes: comparing phospholipid bilayers with monolayer coatings and molecular simulations. Environ Sci Technol 51, 2890–2898. https://doi.org/10.1021/acs.est.6b05662.
[61] Endo, S., Escher, B.I., Goss, K.U., 2011. Capacities of membrane lipids to accumulate neutral organic chemicals. Environ Sci Technol 45, 5912–5921. https://doi.org/10.1021/es200855w.
[62] Çelik, G., Beil, S., Stolte, S., Markiewicz, M., 2022. Environmental hazard screening of heterocyclic polyaromatic hydrocarbons: physicochemical data and in silico models. Environ Sci Technol. https://doi.org/10.1021/acs.est.2c06915.
[63] Spycher, S., Smejtek, P., Netzeva, T.I., Escher, B.I., 2008. Toward a class-independent quantitative structure - Activity relationship model for uncouplers of oxidative phosphorylation. Chem Res Toxicol 21, 911–927. https://doi.org/10.1021/tx700391f.
[64] Willmann, S., Schmitt, W., Keldenich, J., Lippert, J., Dressman, J.B., 2004. A physiological model for the estimation of the fraction dose absorbed in humans. J Med Chem 47, 4022–4031. https://doi.org/10.1021/jm030999b.
[65] Jiang, Z., Gong, X., Wang, B., Wu, Z., Fang, T., 2019. A experimental study on the dehydrogenation performance of dodecahydro-N-ethylcarbazole on M/TiO 2 catalysts. Int J Hydrogen Energy 44, 2951–2959. https://doi.org/10.1016/j.ijhydene.2018.11.236.
[66] Stark, K., Keil, P., Schug, S., Müller, K., Wasserscheid, P., Arlt, W., 2016. Melting points of potential liquid organic hydrogen carrier systems consisting of N-alkylcarbazoles. J Chem Eng Data 61, 1441–1448. https://doi.org/10.1021/acs.jced.5b00679.
[67] Jang, M., Jo, Y.S., Lee, W.J., Shin, B.S., Sohn, H., Jeong, H., et al., 2019. A high-capacity, reversible liquid organic hydrogen carrier: H 2 -Release properties and an application to a fuel cell. ACS Sustain Chem Eng 7, 1185–1194. https://doi.org/10.1021/acssuschemeng.8b04835.
[68] REACH, 1.1.2., Bioaccumulation [WWW Document]; 2023. https://reachonline.eu/reach/en/annex-xiii-1–1.1-1.1.2.html (Accessed 12 May 2023).
[69] Dołżonek, J., Cho, C.W., Stepnowski, P., Markiewicz, M., Thöming, J., Stolte, S., 2017. Membrane partitioning of ionic liquid cations, anions and ion pairs – estimating the bioconcentration potential of organic ions. Environ Pollut 228, 378–389. https://doi.org/10.1016/j.envpol.2017.04.079.
[70] EURAS bioconcentration factor (BCF) Gold Standard Database, (n.d.). https://ambit.sourceforge.net/euras/ (accessed July 28, 2023).
[71] Arnot, J.A., Gobas, F.A.P.C., 2003. A generic QSAR for assessing the bioaccumulation potential of organic chemicals in aquatic food webs. QSAR Comb Sci 22, 337–345. https://doi.org/10.1002/qsar.200390023.
[72] Brzozowski, A.M., Pike, A.C.W., Dauter, Z., Hubbard, R.E., Bonn, T., Engström, O., et al., 1997. Molecular basis of agonism and antagonism in the oestrogen receptor. Nature 389, 753–758. https://doi.org/10.1038/39645.
[73] Takatori, S., Kitagawa, Y., Oda, H., Miwa, G., Nishikawa, J., Nishihara, T., et al., 2003. Estrogenicity of metabolites of benzophenone derivatives examined by a yeast two-hybrid assay. J Health Sci 49, 91–98.
[74] Schultz, T.W., Sinks, G.D., Cronin, M.T.D., 2002. Structure-activity relationships for gene activation oestrogenicity: evaluation of a diverse set of aromatic chemicals. Environ Toxicol 17, 14–23. https://doi.org/10.1002/tox.10027.
[75] Schultz, T.W., Seward, J.R., Sinks, G.D., 2000. Estrogenicity of benzophenones evaluated with a recombinant yeast assay: comparison of experimental and rules-based predicted activity. Environ Toxicol Chem 19, 301–304. https://doi.org/10.1002/etc.5620190208.
[76] Delettré, J., Mornon, J.P., Lepicard, G., Ojasoo, T., Raynaud, J.P., 1980. Steroid flexibility and receptor specificity. J Steroid Biochem 13, 45–59. https://doi.org/10.1016/0022-4731(80)90112-0.
[77] Anstead, G.M., Carlson, K.E., Katzenellenbogen, J.A., 1997. The estradiol pharmacophore: Ligand structure-estrogen receptor binding affinity relationships and a model for the receptor binding site. Steroids 62, 268–303. https://doi.org/10.1016/S0039-128X(96)00242-5.
[78] Fang, H., Tong, W., Branham, W.S., Moland, C.L., Dial, S.L., Hong, H., et al., 2003. Study of 202 natural, synthetic, and environmental chemicals for binding to the androgen receptor. Chem Res Toxicol 16, 1338–1358. https://doi.org/10.1021/tx030011g.
[79] Kawamura, Y., Mutsuga, M., Kato, T., Iida, M., Tanamoto, K., 2005. Estrogenic and anti-androgenic activities of benzophenones in human estrogen and androgen receptor mediated mammalian reporter gene assays. J Heal Sci 51, 48–54. https://doi.org/10.1248/jhs.51.48.
[80] Carstensen, L., Beil, S., Schwab, E., Banke, S., Börnick, H., Stolte, S., 2023. Primary and ultimate degradation of benzophenone-type UV filters under different environmental conditions and the underlying structure-biodegradability relationships. J Hazard Mater 446.
[81] Nakagawa, Y., Suzuki, T., Tayama, S., 2000. Metabolism and toxicity of benzophenone in isolated rat hepatocytes and estrogenic activity of its metabolites in MCF-7 cells. Toxicology 156, 27–36. https://doi.org/10.1016/S0300-483X(00)00329-2.
[82] Combes, R.D., 2000. Endocrine disruptors: a critical review of in vitro and in vivo testing strategies for assessing their toxic hazard to humans. Altern Lab Anim 28, 81–118. https://doi.org/10.1177/026119290002800101.
[83] Tamschick, S., Rozenblut-Koscisty, B., Ogielska, M., Lehmann, A., Lymberakis, P., Hoffmann, F., et al., 2016. Sex reversal assessments reveal different vulnerability to endocrine disruption between deeply diverged anuran lineages. Sci Rep 6 (1), 8. https://doi.org/10.1038/srep23825.